CrossMark
click for updates

View Article Online
View Journal

Journal of Materials Chemistry A

Accepted Manuscript

This article can be cited before page numbers have been issued, to do this please use: Y. LIU, M. Guerrouache, S. I. Kebe, B. Carbonnier and B. Le Droumaguet, *J. Mater. Chem. A*, 2017, DOI: 10.1039/C7TA00410A.

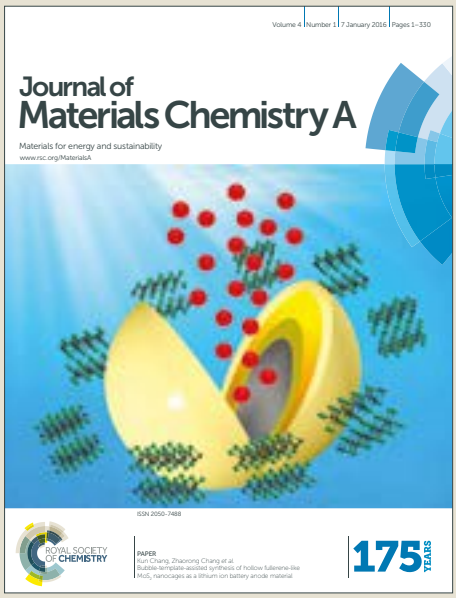

This is an Accepted Manuscript, which has been through the Royal Society of Chemistry peer review process and has been accepted for publication.

Accepted Manuscripts are published online shortly after acceptance, before technical editing, formatting and proof reading. Using this free service, authors can make their results available to the community, in citable form, before we publish the edited article. We will replace this Accepted Manuscript with the edited and formatted Advance Article as soon as it is available.

You can find more information about Accepted Manuscripts in the author guidelines.

Please note that technical editing may introduce minor changes to the text and/or graphics, which may alter content. The journal's standard Terms & Conditions and the ethical guidelines, outlined in our author and reviewer resource centre, still apply. In no event shall the Royal Society of Chemistry be held responsible for any errors or omissions in this Accepted Manuscript or any consequences arising from the use of any information it contains.

ROYAL SOCIETY OF CHEMISTRY

rsc.li/materials-a

View Article Online
DOI: 10.1039/C7TA00410A

Journal Name

ARTICLE

Gold Nanoparticle-Supported Histamine-Grafted Monolithic Capillaries as Efficient Microreactors for Flow through Reduction of Nitro-Containing Compounds†

Received 00th January 20xx,
Accepted 00th January 20xx

DOI: 10.1039/x0xx00000x

www.rsc.org/

Y. Liu,[a] M. Guerrouache,[a] S. I. Kebe,[a] B. Carbonnier[a*] & B. Le Droumaguet[a, *]

Histamine functionalized monolith was synthesized within micro-sized channel as a permeable support for 5, 20 and 100 nm-sized gold nanoparticles immobilization and the resulting nanostructured hybrid monoliths were applied as microreactors for the catalytic reduction of nitro-derivatives. The whole synthetic path of the composite materials relies on (i) UV-induced polymerization of *N*-acryloxysuccinimide and ethylene glycol dimethacrylate in toluene, (ii) surface grafting of histamine through nucleophilic substitution of hydroxysuccinimide leaving groups, and (iii) specific adsorption of citrate-stabilized colloidal gold nanoparticles. The achievement of the successive synthetic steps was ascertained by using a combination of experimental techniques providing information about the chemical composition (FTIR, Raman, EDX), porosity and surface-dispersion of gold nanoparticles (SEM). Of particular interest, it is shown that surface-grafted histamine units exhibit strong affinity towards gold nanoparticles and allow homogeneous and dense dispersion of 5 and 20 nm sized nanoparticles. Consequently, gold nanoparticles size-dependence of the catalytic activity (conversion of nitro and di-nitro aromatic compounds into the corresponding amino and di-amino-derivatives) was demonstrated, highlighting the utmost importance of controlling dispersion of nano-catalysts on support surface, while histamine protonation was also evidenced as a parameter of paramount importance regarding nanogold surface density and thus resulting catalytic activity. Histamine protonation notably allows the generation of electrostatic interaction between citrate-coated gold nanoparticles and thus-formed positive charges at the monolith surface.

Introduction

Nowadays, the development of numerous methods and strategies to design performant microreactors is crucial regarding the constant drive towards miniaturization and high throughput processes, especially in the field of chemistry, biochemistry, biology and nanotechnologies. In this context, polymer-based monolithic reactors have shown a tremendous interest in the past few years as they allow for the preparation of very promising porous materials for flow through applications. Indeed, monoliths can be prepared within microsized channels of fused silica capillaries or chips through simple polymerization pathway starting from a large variety of commercially available functional meth(acrylic) monomers allowing for the fine tuning of their chemical surface characteristics.[1, 2] Of paramount importance, the judicious choice of the chemical nature and amount of porogen(s), the polymerization time along with the crosslinker content in the polymerization feed play a key role and enable finely controlling the size of the channel-like porous structure of monoliths. Moreover, these porous materials are further particularly attractive because of their high chemical stability over a broad range of pH[3] (3 to 10) together with the combination of high permeability and fast mass transport between the monolithic support and the surrounding fluid.[4] Svec research group pioneered the use of such polymer-based monoliths, because of their intrinsic properties (*vide supra*), as stationary phases for chromatographic and electrochromatographic applications.[5] Since then, the technology of monolithic stationary phases has expanded to an unlimited plethora of solutes, regardless of their inherent nature, *i.e.* hydrophobic, hydrophilic, ionic, chiral low molecular weight molecules[3, 6-8], peptides or proteins.[9] Comprehensive and well-documented studies of chemical engineering and separation potentiality of such functionalized polymer monoliths can be found in different reviews in the field, for instance.[10, 11]

However, the major drawback of monoliths relies in their comparatively low surface area relative to silica-based monolithic counterparts that may induce limited separation efficiencies. The surface immobilization of transition or noble metal nanoparticles on monoliths surface has been proposed as an efficient strategy to circumvent this issue. In this respect, gold nanoparticles have particularly attracted much interest from scientists as their synthesis and thiol-mediated surface

[a] Université Paris Est, ICMPE (UMR 7182), CNRS, UPEC, F- 94320 THIAIS France.
E-mail: carbonnier@icmpe.cnrs.fr, ledroumaguet@icmpe.cnrs.fr; Fax: +33 (0)149 78 12 08; Tel: +33 (0)149 78 11 77

† Electronic Supplementary Information (ESI) available: SEM pictures and EDX spectra of monoliths. See DOI: 10.1039/x0xx00000x

This journal is © The Royal Society of Chemistry 20xx

Please do not adjust margins

Published on 21 March 2017. Downloaded by Fudan University on 22/03/2017 03:19:39.

Journal of Materials Chemistry A Accepted Manuscript

View Article Online
DOI: 10.1039/C7TA00410A

Published on 21 March 2017. Downloaded by Fudan University on 22/03/2017 03:19:39.

functionalization are well-described in the literature, as reported in this review from Daniel and Astruc.[12] Additionally, such noble metal nanoparticles are chemically inert towards rather harsh conditions; this may notably ensure their stability in time if one considers routine experiments. The group of Svec notably reported in 2010 on the preparation of monoliths with surface-immobilized gold nanoparticles.[13, 14] Thiol-modified monolithic supports were prepared from a generic poly(glycidyl methacrylate-*co*-ethylene glycol dimethacrylate) monolith through reaction of pendant epoxide moieties with cysteamine. Affinity of gold towards molecules and biomolecules with thiol-functional groups was exploited to the successful separation of peptides and proteins as well as for the capture of cystein containing peptides. The same strategy was implemented for the development of solid phase microextraction method for thiol-containing drugs such as captopril in plasma.[15] Some research groups also clearly demonstrated that the amine functionality allows a full, homogenous and dense covalent attachment of gold nanoparticles as compared to the monolith modified with thiol groups for which the coverage of gold nanoparticles is quite sparse.[16] Cystamine could also be grafted at the surface of generic GMA-based monoliths, reduced to deliver thiol moieties that were used to immobilize GNPs in such a way that these later serve as intermediate ligands for the consequent grafting of hydrophobic thiols, namely mercaptoundecanoic acid and 1-octanethiol. The resulting hybrid monolithic capillaries were successfully used for the separation of diverse proteins in reverse phase-ion exchange mixed mode.[17] More recently, our group discussed a strategy based on UV-driven click reaction to spatially control the deposition of gold nanoparticles on monolith interface.[18] (*N*-acryloxysuccinimide-*co*-ethylene glycol dimethacrylate) monolith was first reacted with propargylamine to provide surface-grafted alkyne groups and further with cysteamine through radical-mediated thiol-yne addition. Photochemical initiation affords spatial control over the reaction site and further chelating properties of the monolith interface. Site-specific immobilization of gold nanoparticles was possible upon simple dynamic loading with gold colloidal solution. The effect of the strategy employed, *i.e. ex situ vs. in situ*, to immobilize GNPs onto amino functionalized monoliths was also carefully investigated regarding the homogeneity and density of GNPs coverage over the monolith pore surface and its influence on catalytic activity towards reduction of *p*-nitrophenol into corresponding *p*-aminophenol.[19] However, flow through catalytic activity of such $-NH_2$ functionalized gold nanoparticle-decorated monoliths was mainly evaluated for supported catalysts prepared *via* the *in situ* strategy involving the chelation of $AuCl_4^-$ as metal-precursor salt, and its subsequent reduction. Indeed, for monolithic catalysts on which were immobilized citrate-stabilized gold nanoparticles some aggregation trends were noticed resulting in clogging of the capillary during the gold nanoparticles deposition step and leading to backpressure increase limiting the range of applicable flow rate for the reduction of nitroaromatic compounds, hence the motivation for this work. Herein, we have focused our investigations on the grafting of suitable ligands at the pore surface of such in-capillary monoliths so as to address this aggregation issue encountered with the *in situ* strategy.

Of particular interest, the immobilization of noble or transition metal nanoparticles, such as gold,[19, 20] platinum[21] or copper,[22] at the pore surface of such polymer-based monolithic capillaries has allowed for the preparation of innovative flow through catalytic microsized reactors during the last years. To extend the progress towards the development of more and more efficient catalytic microsystems, we describe the unprecedented anchoring of an imidazole containing organic ligand, namely histamine, at the surface of polymer-based in-capillary porous material as an efficient chelating group for the robust immobilization of gold nanoparticles on monolith surface. Similarly to the more traditional groups, *i.e.* $-NH_2$[16, 19], $-SH$[13, 14, 23] and $-CN$ [24], histamine provides full, dense and homogeneous dispersion of gold nanoparticles which is a key parameter for taking advantage of the catalytic properties of nanogold. The as obtained nanostructured hybrid monoliths were applied to the reduction of mono- and di-nitro containing aromatic compounds in the presence of $NaBH_4$ as reducing agent.

Experimental

Materials and Methods

N-acryloxysuccinimide (NAS), ethylene glycol dimethacrylate (EDMA), 2,4-dinitroaniline (99%) and 2,6-dinitroaniline (97%) were obtained from Acros Organics (Geel, Belgium). 3-(trimethoxysilyl)propyl methacrylate, 2,5-dinitrophenol (80%), toluene (extra dry), sodium hydroxide (NaOH), hydrochloric acid (HCl) were purchased from Fluka (Isle-d'Abeau, France). HPLC-grade acetonitrile (ACN), ethanol (EtOH, extra dry), histamine (> 97%), *p*-nitrophenol (99%), 3,5-dinitroaniline (97%), colloidal solutions of gold nanoparticles (GNPs) (mean average diameter: 5 nm, 20 nm and 100 nm, stabilized suspensions in citrate buffer) and sodium borohydride ($NaBH_4$) were obtained from Sigma (Isle-d'Abeau, France). 2,2'-azobisisobutyronitrile (AIBN, 98%), purchased from Sigma, was recrystallized from methanol prior to use and stored at –20 °C. All other reagents were used without further purification. Fused silica capillaries with a UV-transparent external coating (75 µm id × 325 µm od) were a kind gift from InnovaQuartz (Phoenix, AZ, USA).

Instrumentation

Functionalization, conditioning steps of the monolithic columns and catalysis were achieved with an HPLC pump (Shimadzu LC-10ATVP, Champs-sur-Marne, France). Spectrolinker XL-1500 UV crosslinker (Spectronics, Westburry, NY, USA) equipped with six lamps (6 × 15 W, 365 nm) was used to photo-initiate the polymerization. UV-Vis spectra were recorded on a Cary 60 UV-Vis Spectrophotometer from Agilent Technologies. Infrared spectra were recorded using a Bruker Tensor 27 DTGS spectrometer in attenuated total reflection (ATR) mode between 4000 and 450 cm^{-1} with an average of 32 consecutive scans and a resolution of 4 cm^{-1}. Morphology of

Journal of Materials Chemistry A Accepted Manuscript

This journal is © The Royal Society of Chemistry 20xx

View Article Online
DOI: 10.1039/C7TA00410A

Published on 21 March 2017. Downloaded by Fudan University on 22/03/2017 03:19:39.

the monolith was evaluated using scanning electron microscopy (SEM) with the help of a MERLIN SEM apparatus (Carl Zeiss, Germany), equipped with Inlens, SE2 and RBSD detectors using a low accelerating tension (from 3 to 10 kV) with a diaphragm aperture of 30 mm. Monolithic capillary columns were cut at different places and small pieces were deposited on a SEM support with a silver containing solution. The samples were dried under reduced pressure and coated with a thin layer of platinum (3 nm) with the help of a Cressington 208 HR sputter-coater (Elektronen Optik Service, Dortmund, Germany). Energy dispersive X-ray spectrometry (EDX) analyses were realized with a AZtec EDS Advanced system (Oxford Instruments society) equipped with a 50 mm^2 SDD X-Max detector ensuring a good energy resolution (127 eV for the manganese Kα ray) using a Inlens detector. Prior to analysis, the samples were coated with a thin layer of palladium (3 nm) with the help of a Cressington 208 HR sputter-coater. Bulk monolith purifications, after functionalization with histamine, were realized on a Sigma 3□15 centrifuge from Sigma Bioblock, operating at 12 000 rpm and rt. for 10 min. Raman spectra were recorded *in situ* on an XPlora One apparatus from Horiba Jobin Yvon equipped with a laser emitting at 638 nm.

Synthetic Procedures

Photopolymerization of poly(NAS-*co*-EDMA) monoliths in capillary. Prior to perform the in situ synthesis of the polymer matrix under UV irradiation, the inner wall of the 100 µm fused silica capillaries was silanized applying the following procedure: (i) fused-silica capillaries were treated with 1 M NaOH for 1 h at room temperature and subsequently heated for 2 h at a temperature of 100 °C. Capillaries were flushed with 0.1M HCl for 15 min, rinsed with deionized water for 15 min and then with acetone for 15 min. Thereafter, capillaries were purged with dry nitrogen gas for 2 h at a temperature of 120 °C. 3-(trimethoxysilyl)propyl methacrylate (30% v/v) solution in toluene was allowed to react overnight with inner silanols at room temperature. At last, the capillaries were rinsed with toluene for 15 min and dried under a stream of nitrogen for 1 h. (ii) The reactive monomer NAS (200 mg) was copolymerized with the crosslinker EDMA (110 µL) in the presence of toluene (700 µL) and AIBN (1% w/w, with respect to the total amount of monomers) as a porogenic solvent and as an initiator, respectively. The mixture was sonicated at room temperature to obtain a homogeneous solution; (iii) thus, the capillary was filled with the reactive mixture, sealed with rubber septa at both ends and irradiated at an overall intensity of 8 $J.cm^{-2}$ for 800 s; (iv) After the photo-polymerization process was completed, the capillary was connected to an HPLC pump for washing with ACN (1 h at a flow velocity of 2 $\mu L.min^{-1}$) to remove the porogen and other soluble compounds that did not react.

Bulk photopolymerization of poly(NAS-*co*-EDMA) monoliths and subsequent functionalization with histamine selector. Organic polymer monolith was synthesized as follows. NAS (200 mg) and EDMA (110 µL) were dissolved in the porogenic solvent, namely toluene (700 µL). Just after the initiator AIBN (1% in mass with respect to the total amount of monomers) was added, the mixture was then irradiated at an overall intensity of 8 $J.cm^{-2}$ for 2 h. After the photopolymerization, the porogenic solvent, *i.e.* toluene, was removed from the P(NAS-*co*-EDMA) monolith by Soxhlet extraction overnight using dichloromethane as extracting solvent; then the white powder was dried under vacuum. Then, to 500 µL of a 1 M histamine solution (111 mg histamine solubilized in 1 mL EtOH) were added to 100 mg of the as-obtained porous P(NAS-*co*-EDMA). The resulting dispersion was stirred at room temperature for 12 h. The dispersion was then centrifuged for 10 min at 12 000 rpm. The supernatant was discarded and the pellet was re-suspended in EtOH. The operation was repeated at least twice to purify the monolith that was finally dried under vacuum. Histamine functionalization was confirmed by FTIR spectroscopy by comparing FTIR monoliths spectra before and after histamine functionalization.

Functionalization of in-capillary poly(NAS-*co*-EDMA) monolith. Chemical modification of the poly(NAS-*co*-EDMA) surface was performed under dynamic conditions at room temperature. Poly(NAS-*co*-EDMA)-filled capillaries were washed with EtOH for 40 min, the monolithic columns were then allowed to react with EtOH solutions of histamine (1 M) for 1 h. Thereafter the monolithic columns were washed with EtOH for 15 min in order to remove the unreacted histamine.

Immobilization of gold nanoparticles on the monolith surface. The monolith was then rinsed with HCl to protonate the grafted imidazole moieties. The adsorption of GNPs was performed upon dynamic loading (2 $\mu L.min^{-1}$) of colloidal solutions containing 5, 20 or 100 nm GNPs and it was considered complete when the liquid coming out from the capillary column appeared in its original color. The specific role of the imidazole surface functionality in the GNPs immobilization was initially ascertained by simple visual observation of the monolithic capillary column. The color of the histamine-functionalized monolith became dark purple upon adsorption of GNPs and the color remained upon thorough rinsing with water. The capillary grafted GNPs were then used for heterogeneous organometallic catalysis, namely for the reduction of nitro aromatic compounds.

Reduction of nitro- and dinitroaromatic compounds by organometallic heterogeneous catalysis by in-capillary GNPs functionalized histamine-grafted monoliths. A freshly prepared solution containing 200 µL of *p*-nitrophenol (5 mg in 10 mL EtOH), 200 µL of $NaBH_4$ (114 mg in 10 mL EtOH) in 4 mL EtOH was injected in the 20 µL loop of an HPLC pump system, the solution coming out from the in-capillary GNPs functionalized histamine-grafted monoliths was collected and analyzed by UV spectrophotometry. The same protocol was repeated for the supported nanogold-mediated catalytic reduction of 2,4-dinitroaniline, 3,5-dinitroaniline, 2,5-dinitroaniline and 2,5-dinitrophenol.

Journal of Materials Chemistry A Accepted Manuscript

Please do not adjust margins

View Article Online
DOI: 10.1039/C7TA00410A

Published on 21 March 2017. Downloaded by Fudan University on 22/03/2017 03:19:39.

Results & Discussion

In capillary monoliths preparation and characterization

A straightforward two-step process was necessary for preparing a histamine-grafted porous monolith within a fused silica capillary (inner diameter = 75 µm), as shown on **Scheme 1**. After activation of the inner wall of the capillary in the presence of 3-(trimethoxysilyl)propyl methacrylate so as to tightly anchor the monolith into the capillary (**Fig. S1**, **ESI**), a reactive monomer, *i.e. N*-acryloxysuccinimide (NAS), was copolymerized with a cross-linking comonomer, namely ethylene glycol dimethacrylate (EDMA) in the presence of a radical initiator (2,2'-azobisisobutyronitrile, 1% w/w, with respect to the total amount of monomers) and a porogenic solvent (toluene). Upon filling the pre-activated capillary with this polymerization mixture, sealing of the capillary extremities with rubber septa and subsequent photo-initiated copolymerization within a UV oven, an in-capillary P(NAS-*co*-EDMA) monolith was obtained with nucleophilic-sensitive *N*-hydroxysuccinimide activated ester functionalities. The presence of well-defined interconnected pores in the micrometer-size range was demonstrated by the white optical appearance of the capillary, suggesting the occurrence of flow-through channels with dimensions in the same order of magnitude than that of visible light wavelength, *i.e.* in the micrometer range, as already observed in previous studies.[3, 8, 9, 18, 19, 22] This observation was also corroborated by scanning electron microscopy (SEM) of the porous material that displayed a homogeneous monolithic morphology constituted of interconnected ~1-2 µm-sized globules (**Fig. 1**) all along the capillary length with interconnected pores in the few micrometers range that allow for sufficient permeability and thus fast mass transport. The monolith was also prepared in bulk so as to further confirm the covalent grafting of histamine at the monolith interface *via* Fourrier Transform Infrared (FTIR) spectroscopy.

Functionalization of the NAS-based monolithic columns with histamine

The immobilization of GNPs on monolithic capillary has been in the past achieved on monoliths on which were tethered either amine,[16, 18] nitrile[24] or thiol functionalities.[13, 14, 16, 23] On the other hand, histamine, likely due to its imidazole ring, has been shown to interact very tightly with metal ions, but, to the best of our knowledge, some evidence of metallic nanoparticles adsorption to this chemical graft has never been clearly evidenced, even if some studies hypothesized it.[25]

Imidazole can indeed generate two types of molecular interactions: π-π interactions due to its aromatic ring and electrostatic interactions due to amino groups, providing that the pH is suitably chosen.[26]

In our strategy, histamine was selected as a ligand of choice as it should allow facile adsorption of citrate-stabilized preformed GNPs through electrostatic interaction between positively charged ammonium moieties of histamine and negatively charge carboxylate groups of citrate stabilizing agent coating GNPs. In consequence, flushing a 1 M histamine solution in EtOH through the P(NAS-*co*-EDMA) capillary was realized and allowed quantitative consumption of the *N*-hydroxysuccinimide activated ester functions of the monolith, thus allowing for the formation of covalent amide bond with the terminal aliphatic amine moiety of histamine.

This was ascertained by FTIR spectroscopy of the as-obtained bulk monolith. Indeed, vanishing of the NAS characteristic peaks at 1810 and 1780 cm^{-1} was observed together with the appearing of new signals assigned to the aromatic imidazole ring (1645, 1565, 1450 and 1380 cm^{-1}) and to –NH stretching band of the amine (3210 cm^{-1}) functions, as shown on **Fig. 2**, thus demonstrating the success of the functionalization step.

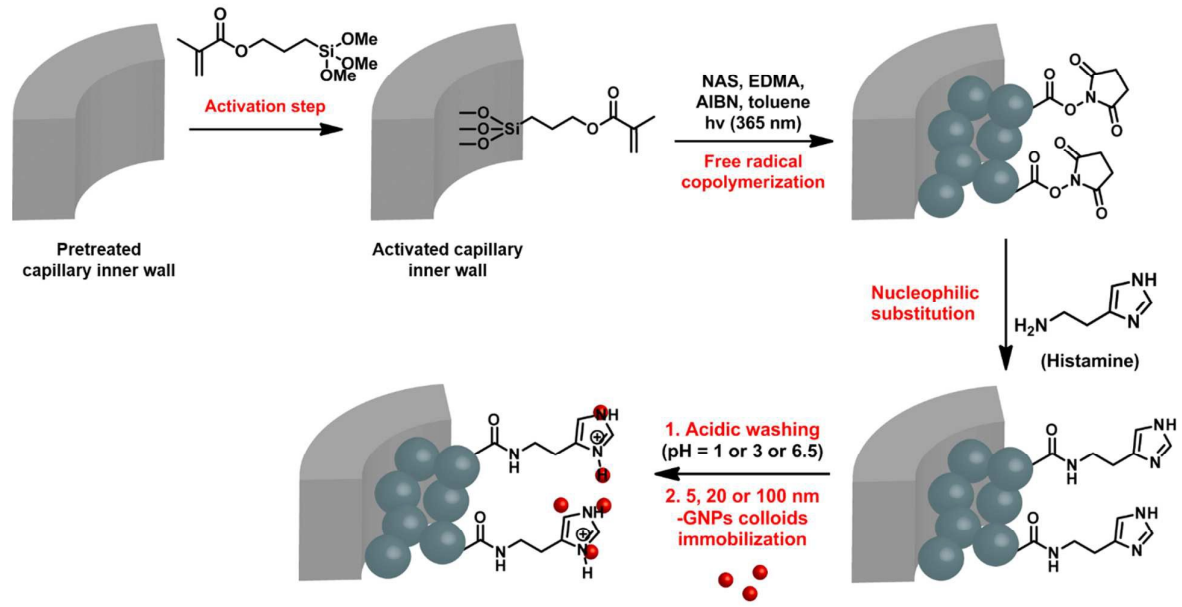

This journal is © The Royal Society of Chemistry 20xx

Please do not adjust margins

Journal of Materials Chemistry A Accepted Manuscript

View Article Online
DOI: 10.1039/C7TA00410A

Scheme 1. Synthetic pathway followed for preparing GNPs surface-immobilized porous polymeric monoliths via free radical photo-initiated copolymerization, histamine grafting and gold nanoparticles adsorption. The scheme is not to scale as the spheres corresponding to gold nanoparticles represent size in the 5-100 nm (depending on the size of GNPs adsorbed at the monolith pore surface) that is much smaller than the size of monolith globules.

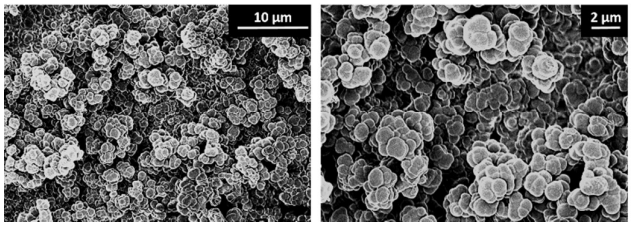

Fig. 1. Scanning Electron Micrographs of a cross-section of the NAS-based monolithic capillary.

It is worth mentioning that a dramatic decrease of the carbonyl peak was also noticed at 1730 cm^{-1}. This can be easily explained by the nucleophilic substitution of surface NHS activated esters with primary amine of histamine that release *N*-hydroxysuccinimide. Compared with pristine monolith, the histamine-functionalized one presents much less carbonyl moieties, thus explaining the dramatic decrease of the carbonyl peak.

This finding was also corroborated by *in situ* Raman spectroscopy by comparing spectra of the pristine NAS-based monolithic capillary obtained before and after grafting reaction. It clearly demonstrated the dramatic decrease of the peaks arising from NAS moiety after the reaction at 1815 cm^{-1} (activated ester stretching), 1790 cm^{-1} (imide symmetric stretching) and 1730 cm^{-1} (imide asymmetric stretching), respectively.[8, 18, 27, 28] Finally, another peak corresponding to the –N-H amine stretching of imidazole ring also appeared at 3125 cm^{-1} after functionalization with histamine. It is worth mentioning that the porous morphology of the resulting histamine functionalized in-capillary monolith remained unchanged after this functionalization step (data not shown).

In addition, EDX semi-quantitative analyses of the in-capillary monolith before and after histamine grafting confirmed FTIR and *in situ* Raman results. As observed on the **Fig. 3**, a significant 3-fold increase in the nitrogen content (% w/w as compared to the total amount of C, N and O elements) of the resulting monolith was evidenced, likely due to histamine grafting onto the P(NAS-*co*-EDMA) pore surface.

Prior to GNPs adsorption at the pore surface of the capillary, the P(NAS-*co*-EDMA) monolith was also subjected to a rinsing step with an acidic aqueous solution at pH = 1 or 3 in order to protonate the available nitrogen lone pair of the aromatic imidazole ring of histamine whose pKa was evaluated at 5.8 in previous studies.[29] This notably allowed to study the influence of the chemical nature of the interface over gold nanoparticle immobilization.

Immobilization of gold nanoparticles on histamine-functionalized monolithic capillaries

The immobilization of GNPs on the histamine-functionalized polymeric porous monolith was achieved upon dynamic loading of a gold colloidal suspension through the capillary. In order to study the influence of the acidic rinsing step and thus of the chemical nature of the polymeric interface regarding the adsorption of GNPs, a commercial 20 nm sized nanogold colloid was flushed through histamine functionalized in-capillary monolith preliminary rinsed at pH = 6.5, 3 or 1.

This successfully allowed for the adsorption of gold nanoparticles at the pore surface within 12 h, as immediately observed to the naked eye (**Fig. S2, ESI**) with the appearing of a homogeneous dark purple coloration all along the capillary for pH 3 and 1 while only a faint pink color was observed with the capillary rinsed with pH 6.5 aqueous solution. To the best of our knowledge, this is actually the first time that chelating properties of histamine selector towards stabilized GNPs is clearly demonstrated. This GNPs adsorption was also confirmed by SEM imaging and EDX spectroscopy (**Fig. 4 and Table 1, entry 2 & 3**). In both cases (pH = 3 or 1), a dense and homogeneous 20 nm GNPs coverage over histamine-grafted P(NAS-*co*-EDMA) monolith was immediately noticed by SEM (**Fig. 4**). More interestingly, the monolith rinsed with pH 1 HCl aqueous solution showed a denser gold nanoparticle coverage than the monolith rinsed with pH 3 HCl solution. Quantification of gold by EDX analysis in both hybrid monoliths confirmed this findings (**Table 1**, **entry 2 & 3**).Indeed, a much higher gold content was observed when the capillary was subjected to acidic washings at pH 1 (17.04 ± 4.03 wt. %) than at pH 3 (9.69 ± 1.08 wt. %), prior to GNP immobilization. These results are in the same order of magnitude than those already reported in the literature for the immobilization of gold nanoparticles over polymeric monolith, *i.e.* in the 15-60 wt. % range.[16, 23]

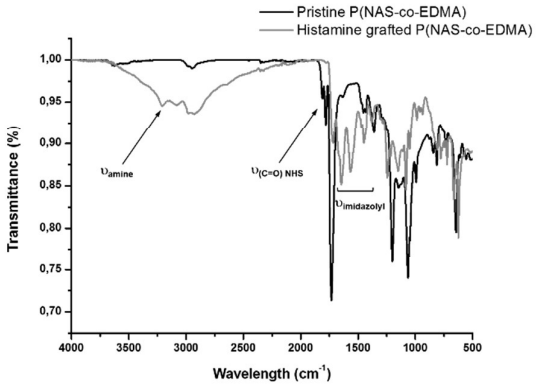

Fig. 2. FT-IR spectra of the P(NAS-*co*-EDMA) bulk pristine monolith before (black curve) and after (grey curve) functionalization with histamine.

Published on 21 March 2017. Downloaded by Fudan University on 22/03/2017 03:19:39.
Journal of Materials Chemistry A Accepted Manuscript

Please do not adjust margins

View Article Online
DOI: 10.1039/C7TA00410A

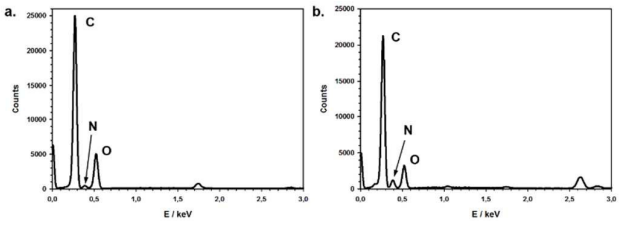

Fig. 3. EDX spectra of in-capillary P(NAS-*co*-EDMA) monolith before (a) and after (b) functionalization step with histamine.

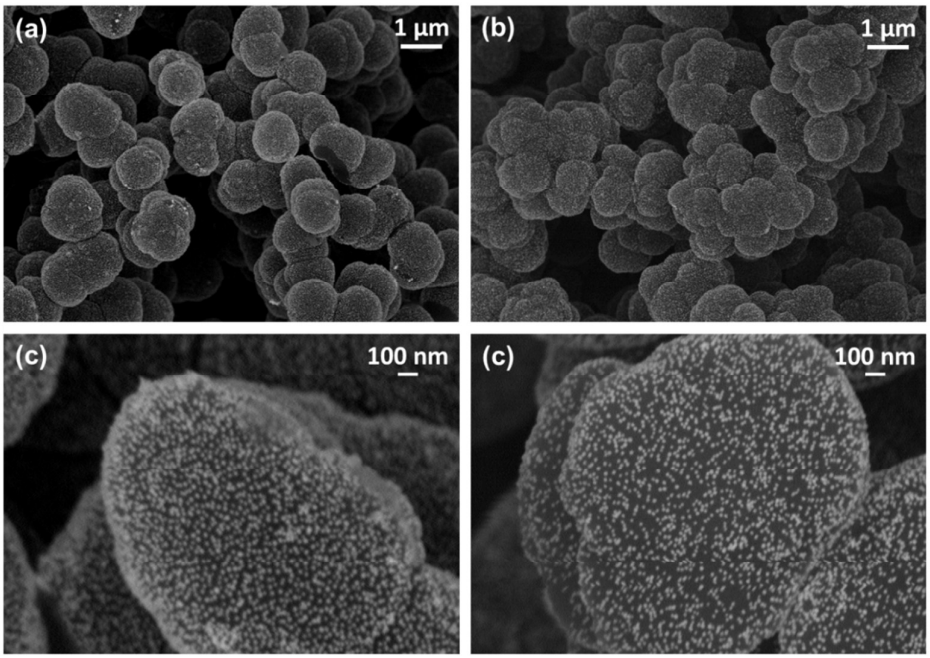

Fig. 4. SEM images of a cross-section of the 20 nm GN*P*-based hybrid monoliths realized upon rinsing at pH = 1 (a, c) or pH = 3 (b, d), prior to GNPs adsorption. The white spots represent gold nanoparticles.

Table 1. Semi-quantitative determination of wt. % content of the different adsorbed gold nanoparticles monoliths as determined by EDX analysis.

Sample	%wt C[a]	%wt O[a]	%wt Au[a]
monolith@5nm GNPs pH 1	68.45 ± 7.52	27.89 ± 9.03	3.66 ± 2.61
monolith@20nm GNPs pH 1	62.90 ± 4.28	20.10 ± 0.48	17.04 ± 4.03
monolith@20nm GNPs pH 3	74.31 ± 2.09	15.99 ± 3.09	9.69 ± 1.08
monolith@20nm GNPs pH 6.5	81.64 ± 1.77	14.38 ± 2.52	3.98 ± 0.77
monolith@100nm GNPs pH 1	47.44 ± 13.36	9.96 ± 2.47	42.61 ± 15.06

[a] Mean average C, O and Au content (wt. %) were determined on 3 distinct cross-sections of the hybrid monolithic capillaries.

Accordingly to previous results, the gold content of the hybrid capillary stemming from the monolith rinsed with pH 6.5 aqueous solution was found to be as low as 3.98 wt. %.

Both techniques clearly pointed out the crucial role of the pH solution during the rinsing step prior to GNPs adsorption and thus the importance of histamine protonation over GNPs adsorption. This can be also verified on the EDX spectra in **Fig. S4, ESI** in which a clear difference is observed in the gold content upon immobilization of 20 nm sized gold nanoparticles after either rinsing at pH 1 or 3. XPS spectra of the bulk citrate-stabilized 20 nm-sized GNP immobilized histamine-functionalized hybrid microcolumns were also realized (**Fig. S6, ESI**). Only that arising from the monolith preliminarily rinsed with a pH 1 aqueous solution showed clearly visible characteristic signals from gold with Au $4f_{7/2}$ and Au $4f_{5/2}$ peaks at 83.5 and 87.4 keV, respectively.

This can be easily explained by electrostatic interactions that take place between the positively charged monolith interface and negatively charged citrate-stabilized GNPs, thus highlighting the crucial role of both citrate and ammonium groups regarding the immobilization of GNPs, as already reported in a previous study.[19] In addition, SEM investigation demonstrated that this rinsing step was not destructive towards the monolith structure, methacrylate-based monoliths being inert in a broad range of pHs. Consequently, the rinsing step of the histamine-functionalized monolith was further realized at pH = 1 in order to improve metallic nanoparticles immobilization on the functional porous

This journal is © The Royal Society of Chemistry 20xx

Please do not adjust margins

Published on 21 March 2017. Downloaded by Fudan University on 22/03/2017 03:19:39.

Journal of Materials Chemistry A Accepted Manuscript

View Article Online
DOI: 10.1039/C7TA00410A

material. In the same manner, the influence of GNPs diameter over monolith coverage was further investigated. In this purpose, 5 nm GNPs colloids were flushed through the histamine functionalized P(NAS-*co*-EDMA) capillary preliminary rinsed at pH 1. It only allowed a weak coverage of the pore surface of the monolith as shown on **Fig. 5a**, even if the immobilization along the entire capillary was achieved within 4 h. Unfortunately, a much lower gold content, *i.e.* 3.66 ± 2.61 wt. %, was found by EDX semi-quantitative analysis. As observed by SEM (**Fig. 5c**), a disperse coverage of the histamine grafted monolith was noticed in the case of 100 nm GNPs along with some aggregation patterns (**Fig. S3, ESI**). This was also confirmed by EDX analysis that pointed out a great variation of the gold content of the hybrid monolith, notably depending on the area on which the analysis was realized, *i.e.* in GNPs aggregation areas or in less densely distributed areas (**Fig. S5, ESI**). Nonetheless, an average gold content of 42.61 ± 15.06 wt. % could be calculated, even though a great standard variation on the measurement was observed. In addition, the 100 nm GNP adsorption step was much more difficult at the pore surface of such monoliths as only nearly 3 cm of the capillary was decorated with GNPs after 48h. This demonstrated the crucial role of the GNP size over the coverage density on the porous polymeric surface, and thus on the gold specific surface area increasing. Indeed, as observed in **Fig.5b**, 20 nm GNPs seem more suitable than 5 and 100 nm GNPs as derivatives in the presence of $NaBH_4$. They allowed for obtaining dense GNP distribution while avoiding any aggregation phenomena.

Flow through supported catalysis within hybrid microcolumns

Immobilized GNPs are prone to act as organometallic catalysts in various reactions, among which the reduction of nitroaromatic compounds to the corresponding amino. In this work, we thus decided to focus our attention on this particular supported GN*P*-mediated catalytic reaction.

Published on 21 March 2017. Downloaded by Fudan University on 22/03/2017 03:19:39.
Journal of Materials Chemistry A Accepted Manuscript

Please do not adjust margins

View Article Online
DOI: 10.1039/C7TA00410A

Published on 21 March 2017. Downloaded by Fudan University on 22/03/2017 03:19:39.

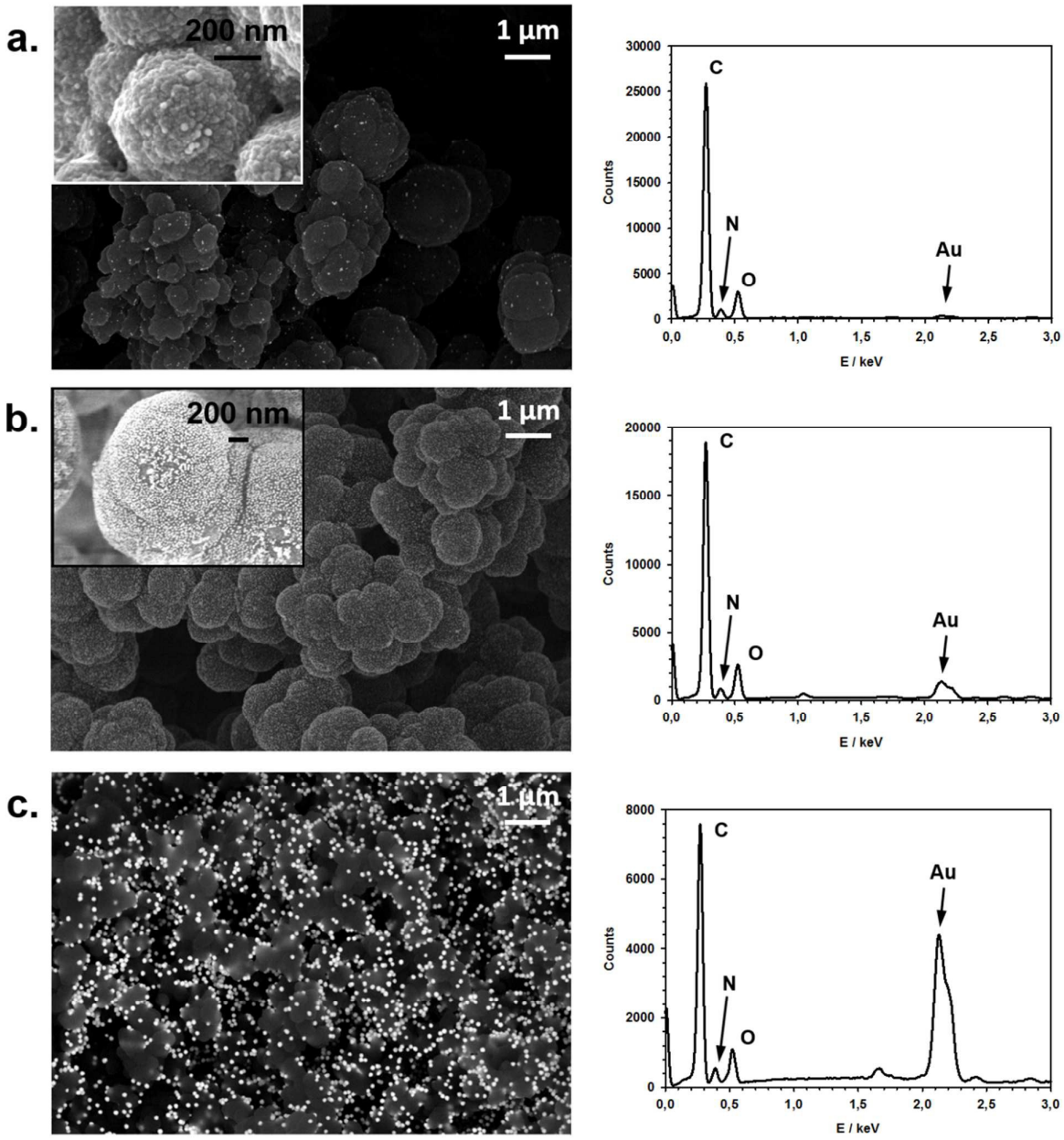

Fig. 5. SEM images (RBSD detector, left) and corresponding EDX spectra (right) of (a) 5 nm GNPs-, (b) 20 nm GNPs- and (c) 100 nm GNPs-adsorbed histamine-grafted monolith interfaces. Insets show higher magnification micrographs of the 5-nm and 20-nm GNPs immobilized hybrid materials realized with Inlens detector. The white spots on SEM images represent GNPs

To this purpose, a solution of *p*-nitrophenol and $NaBH_4$ in EtOH was injected in a 7 cm length 5 nm GNPs immobilized hybrid monolithic capillaries at increasing flowrates, namely 2 and 5 $\mu L.min^{-1}$. An excess of $NaBH_4$ was used in our experimental procedure. Accordingly, the reduction of such nitrocompounds over supported GNPs do not depend on the concentration of this reducing agent.[30, 31] The eluting yellowish solution constituted of *p*-nitrophenol and $NaBH_4$ injected at the inlet of the GNPs-supported monolithic capillary was found totally faded at the outlet, thus suggesting a total conversion of the nitro compound into the corresponding amino compound. We thus decided to collect the eluted solution at the outlet of the capillary and to analyze it by UV-visible spectroscopy. It was immediately observed that the characteristic band of *p*-nitrophenolate at 400 nm decreased when the solution was passed through GNPs immobilized hybrid capillary. The conversion of each catalytic reaction was calculated by comparing the absorbance of the solution before and after nanometal-catalyzed reaction in the hybrid microcolumn at a wavelength corresponding to the π→π*transition peak of the

Journal of Materials Chemistry A Accepted Manuscript

Please do not adjust margins

View Article Online
DOI: 10.1039/C7TA00410A

Published on 21 March 2017. Downloaded by Fudan University on 22/03/2017 03:19:39.

reactant, *i.e.* (di)nitroaromatic compound. It is worth mentioning that for each reaction, a negative blank in which the nitro-compound was injected in a histamine-grafted monolith was used as a negative control. In this way, it was also possible to prove that the presence of supported GNPs is necessary for the catalytic reaction to occur and that no dilution affects the absorbance of the nitro-based reagent or amino-based product. More interestingly, it was noticed that decreasing the flowrate of the HPLC pump allowed for a better conversion of the nitroaromatic compound, as demonstrated by the dramatic decrease of the characteristic π→π* band of *p*-nitrophenolate ion at 400 nm (**Fig. 6.a**) in the case of 5 nm immobilized GNPs and a strong increase of the π→π* band of *p*-aminophenolate at 300 nm. Conversions of 53% and 64% were thus obtained with immobilized 5 nm-sized GNPs hybrid microcolumns for flowrates of 0.5 and 0.2 $\mu L.min^{-1}$, respectively. This can be easily explained by longer contacts between nanogold and reagents at lower flowrates, thus enabling higher nitro reduction yields.

Further, the GNP size effect was investigated by comparing two different hybrid capillary columns, namely those prepared after immobilization of 5 nm or 20 nm GNPs on the histamine grafted monolith. As expected, it immediately demonstrated the better efficacy of the 20 nm GNPs immobilized column over the 5 nm one. Indeed, when the same flowrate was used for both columns, *i.e.* 5 $\mu L.min^{-1}$, the conversion of the *p*-nitrophenol into the corresponding amino-containing compound was virtually quantitative when using hybrid monolithic column generated with 20 nm GNPs (**Fig. 6.b**). As aforementioned, in the case of immobilized 5 nm GNPs, the reduction yield was found to be only 53% by comparing the absorbance of the negative control with those of the GNPs-mediated reaction. However, when comparing the conversion obtained from hybrid monolithic columns generated with 5 and 20 nm GNPs as a function of the gold content in the column, it is obvious that 5 nm GNPs immobilized hybrid capillaries show better conversions (53% conversion for 3.66 wt. % in the case of 5 nm GNPs vs. 99% conversion for 17.04 wt. % in the case of 20 nm GNPs). Thus the surface to volume ratio is more favorable in the case of 5 nm GNPs and allows a higher surface contact with reactants, leading to higher conversions. Besides dense coverage of the histamine-grafted monolith interface with 100 nm GNPs, a high back pressure and even clogging of the capillary in some cases did not allow for using such microsystems in the hydride-mediated reduction of nitro-containing aromatic compounds, explaining the lack of results with this system.

To demonstrate the recyclable character of the hybrid capillary columns, the same flow through catalytic reaction was repeated 5 times in a row with the hybrid in-capillary monolith obtained after immobilization of 20 nm GNPs. conversions up to 96 % after 5 cycles demonstrated the possibility to use such hybrid systems for repeated processes.

Furthermore, we investigated the possibility to reduce di-nitro aromatic compounds with such prepared 20 nm GNPs-immobilized hybrid monoliths.

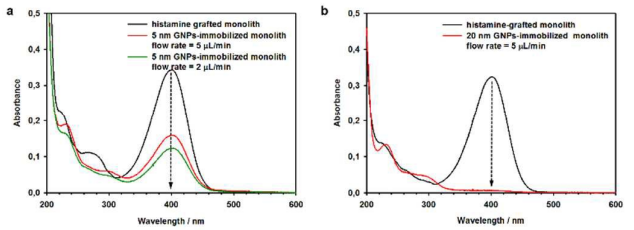

Fig. 6. UV spectra of *p*-nitrophenol solution supplemented with $NaBH_4$ after flushing through histamine grafted P(NAS-*co*-EDMA) capillary ((a) and (b), black curve), through 5 nm GNPs immobilized capillary at a 5 $\mu L.min^{-1}$ ((a), red curve) or at a 2 $\mu L.min^{-1}$ flowrate ((a), green curve) or through 20 nm GNPs immobilized capillary at a 5 $\mu L.min^{-1}$ flowrate ((b), red curve). Capillaries were all 7 cm length and the pump flowrate was varied from 2 to 5 $\mu L.min^{-1}$.

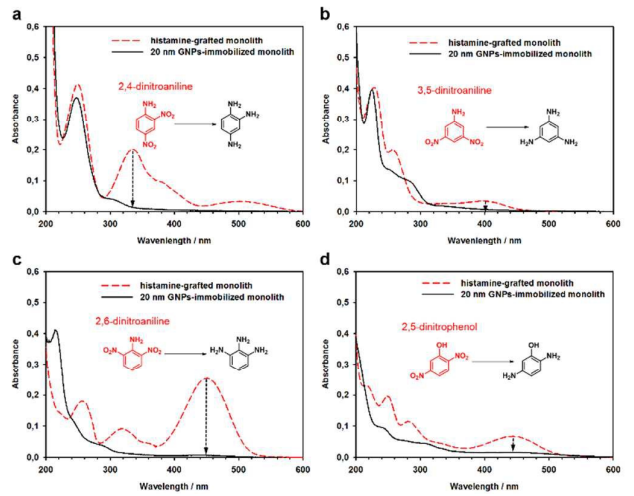

Fig. 7. UV spectra of (a) 2,4-dinitroaniline, (b) 3,5-dinitroaniline, (c) 2,6-dinitroaniline and (d) 2,5-dinitrophenol upon flushing through histamine-grafted monolith (red curve) or 20 nm GNPs-immobilized monolith (black curve). Capillaries were all 7 cm length and the pump flowrate was fixed at 5 $\mu L.min^{-1}$.

For this purpose, a series of 4 dinitroaromatic compound was selected: 2,4-dinitro-, 3,5-dinitro-, 2,6-dinitroaniline and 2,5 dinitrophenol. As shown in **Fig. 7**, the hybrid capillary column exhibited good catalytic activity with excellent yields toward this series of dinitroaromatic compounds regardless of the nature and position of the substituents on the aromatic ring.

Indeed, after recovery of each solution at the capillary outlet and *ex situ* analysis by UV-visible spectroscopy, a quantitative reduction was observed as demonstrated by the vanishing of the characteristic band ascribed to the π → π* electronic transition of these dinitro- compounds, as indicated by a dashed arrow.

Conclusions

In this contribution, we have proposed the surface-grafting of a naturally-occurring amine, *i.e.* histamine, onto *N*-hydroxy-succinimide-functionalized monolith with the aim to produce nanostructured monoliths acting as microreactors for the catalytic reduction of nitroaromatic derivatives. As demonstrated in this work, two crucial parameters have to be

Journal of Materials Chemistry A Accepted Manuscript

Please do not adjust margins

View Article Online
DOI: 10.1039/C7TA00410A

seriously taken into consideration for the rational design of such catalytically active hybrid materials, *i.e.* the average diameter of the nanometal colloid and the nature of the porous material interface. In this particular case, best results in terms of permeability and nanometal content were obtained with 20 nm GNPs and highly positively charged interface. For the 20 nm sized particles, homogeneous and dense surface dispersion of the metallic colloid was obtained. The gold content of the resulting hybrid monolith was estimated by EDX analysis and found to be as high as 17 wt. %. The proposed approach is proved to be a promising method for complete conversion of reactants within a few minutes within short hybrid monolithic capillaries. Such hybrid capillary columns could thus be easily envisionned for facile screening of catalytic reactions, regardless of the nature of the transition or noble metal used. Moreover, it can be extended to other types of chemical reaction as well as other nanometals. Besides, the adsorption of such GNPs onto the porous monolith surface may enable to increase the specific surface area of such monoliths and thus the interactions with solutes for capillary (electro)chromatography for instance. Finally, another prospect of such hybrid capillaries relies on the reduction and consecutive quantification of trinitrotoluene (TNT), the systems being thus used for the qualitative as well as quantitative analysis of this explosive.

Acknowledgements

The authors wish to acknowledge the Université Paris-Est and CNRS for financially supporting this research. S. I. K. is grateful to the Ministry of Higher Education and Scientific Research of the Government of Senegal for financial funding during his PhD. We would also like to thank Rémy Pirès for his assistance in the SEM/EDX microscopy measurements.

Notes and references

1 M. R. Buchmeiser, *Polymer*, 2007, **48**, 2187.
2 F. Svec, *J. Chromatogr. A*, 2010, **1217**, 902.
3 M. Guerrouache, A. Pantazaki, M.-C. Millot and B. Carbonnier, *J. Sep. Sci.*, 2010, **33**, 787.
4 A. E. Rodrigues, J. C. Lopes, Z. P. Lu, J. M. Loureiro and M. M. Dias, *J. Chromatogr. A*, 1992, **590**, 93.
5 F. Svec and J. M. J. Frechet, *Anal. Chem.*, 1992, **64**, 820.
6 M. Lämmerhofer, F. Svec, J. M. J. Fréchet and W. Lindner, *J. Chromatogr. A*, 2001, **925**, 265.
7 Z. Jiang, N. W. Smith, P. D. Ferguson and M. R. Taylor, *Anal. Chem.*, 2007, **79**, 1243.
8 M. Guerrouache, M.-C. Millot and B. Carbonnier, *Macromol. Rapid Commun.*, 2009, **30**, 109.
9 B. Carbonnier, M. Guerrouache, R. Denoyel and M.-C. Millot, *J. Sep. Sci.*, 2007, **30**, 3000.
10 S. Eeltink and F. Svec, *Electrophoresis*, 2007, **28**, 137.
11 M. Guerrouache, A. M. Khalil, S. Kebe, B. L. Droumaguet, S. Mahouche-Chergui and B. Carbonnier, *Surf. Innovations*, 2015, **3**, 84-102.
12 M. C. Daniel and D. Astruc, Chem. Rev., 2004, 104, 293-346.
13 Y. Xu, Q. Cao, F. Svec and J. M. J. Fréchet, *Anal. Chem.*, 2010, **82**, 3352.
14 Q. Cao, Y. Xu, F. Liu, F. Svec and J. M. J. Fréchet, *Anal. Chem.*, 2010, **82**, 7416.
15 A.-Z. Zhang, F.-G. Ye, J.-Y. Lu, Z. Wei, Y. Peng and S.-L. Zhao, *Chin. J. Anal. Chem.*, 2011, **39**, 1247.
16 D. Connolly, B. Twamley and B. Paull, *Chem. Commun.*, 2010, **46**, 2109.
17 L. Terborg, J. C. Masini, M. Lin, K. Lipponen, M.-L. Riekolla and F. Svec, *J. Adv. Res.*, 2015, **6**, 441.
18 M. Guerrouache, S. Mahouche-Chergui, M. M. Chehimi and B. Carbonnier, *Chem. Commun.*, 2012, **48**, 7486.
19 A. M. Khalil, V. Georgiadou, M. Guerrouache, S. Mahouche-Chergui, C. Dendrinou-Samara, M. M. Chehimi and B. Carbonnier, *Polymer*, 2015, **77**, 218.
20 P. Floris, B. Twamley, P. N. Nesterenko, B. Paull and D. Connolly, *Microchim. Acta*, 2013, **181**, 249.
21 R. Poupart, D. Nour El Houda, D. Chellapermal, M. Guerrouache, B. Carbonnier and B. Le Droumaguet, *RSC Adv.*, 2016, **6**, 13614.
22 R. Poupart, B. Le Droumaguet, M. Guerrouache and B. Carbonnier, *Mater. Chem. Phys.*, 2015, **163**, 446.
23 Y. Lv, F. M. Alejandro, J. M. J. Fréchet and F. Svec, *J. Chromatogr. A*, 2012, **1261**, 121.
24 K. C. Grabar, R. G. Freeman, M. B. Hommer and M. J. Natan, *Anal. Chem.*, 1995, **67**, 735.
25 M.-C. Saada, J.-L. Montero, D. Vullo, A. Scozzafava, J.-Y. Winum and C. T. Supuran, *J. Med. Chem.*, 2011, **54**, 1170.
26 G. Kaştaş, H. Paşaoğlu and B. Karabulut, *Polyhedron*, 2011, **30**, 2599.
27 M. Guerrouache, S. Mahouche-Chergui, T. Mekhalif, T. T. H. Dao, M. M. Chehimi and B. Carbonnier, *Surf. Interface Anal.*, 2014, **46**, 1009.
28 I. Tijunelyte, J. Babinot, M. Guerrouache, G. Valincius and B. Carbonnier, *Polymer*, 2012, **53**, 29.
29 K. B. Kim, J.-H. Han, H. Choi, H. C. Kim and T. D. Chung, *Small*, 2012, **8**, 378.
30 K. Kuroda, T. Ishida and M. Haruta, *J. Mol. Catal. A-Chem.*, 2009, **298**, 7.
31 Y. Ye, M. Jin and D. Wan, *J. Mater. Chem. A*, 2015, **3**, 13519.

Published on 21 March 2017. Downloaded by Fudan University on 22/03/2017 03:19:39.
Journal of Materials Chemistry A Accepted Manuscript

This journal is © The Royal Society of Chemistry 20xx

View Article Online
DOI: 10.1039/C7TA00410A

Published on 21 March 2017. Downloaded by Fudan University on 22/03/2017 03:19:39.

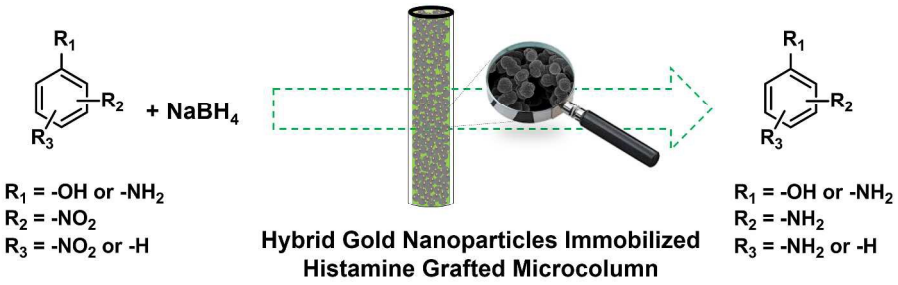

600x300mm (150 x 150 DPI)

Journal of Materials Chemistry A Accepted Manuscript